Applied Geochemistry 63 (2015) 10–21

Contents lists available at ScienceDirect

Applied Geochemistry

journal homepage: www.elsevier.com/locate/apgeochem

Identification of spatio-seasonal hydrogeochemical characteristics of the unconfined groundwater in the Red River Delta, Vietnam

Thuy Thanh Nguyen [a, *], Akira Kawamura [a], Thanh Ngoc Tong [b], Hideo Amaguchi [a], Naoko Nakagawa [a], Romeo Gilbuena Jr. [a], Duong Du Bui [b]

[a] Department of Civil and Environmental Engineering, Tokyo Metropolitan University, 1-1 Minami-Oshawa, Hachioji, Tokyo, 192-0397, Japan
[b] Center of Water Resources Planning and Investigation, Ministry of Natural Resources and Environment, Hanoi, Viet Nam

ARTICLE INFO

Article history:
Received 2 June 2014
Received in revised form
23 July 2015
Accepted 25 July 2015
Available online 31 July 2015

Keywords:
Hydrogeochemistry
Groundwater
Self-organizing maps
Unconfined aquifer
The Red River Delta

ABSTRACT

Groundwater has been the primary source of daily water supplies for people living in the Red River Delta, the second largest delta in Vietnam. For this reason, identification of hydrogeochemical properties of the groundwater is indispensable for sustainable utilization of groundwater sources. In this study, the spatio-seasonal hydrogeochemical characteristics of groundwater in the unconfined aquifer of the Red River Delta have been investigated by systematically applying self-organizing maps (SOM) and Gibbs diagrams. The groundwater chemistry dataset used in the analysis is composed of eight major dissolved ions (i.e., Ca^{2+}, Mg^{2+}, Na^{+}, K^{+}, HCO_3^{-}, Cl^{-}, SO_4^{2-}, and CO_3^{2-}) and total dissolved solids that are collected from 47 groundwater monitoring wells within the study area during the dry and rainy seasons. The SOM application classified the hydrogeochemical data into five clusters, which revealed three basic representative water types: high salinity (one cluster), low salinity (two clusters), and freshwater (two clusters). The spatial distribution of clusters and water types were identified. In particular, the low-salinity type was found not only in the downstream area but also in the northeastern parts of the upstream and middle-stream areas, where the groundwater was mainly classified into one specific cluster, in which agricultural activities were considered to influence groundwater chemistry. Cluster changes from the dry to rainy seasons were detected in approximately one-fifth of the observations wells. Dilution by surface water may significantly affect the chemical characteristics of the unconfined aquifer during the rainy season. Based on Gibbs diagrams, rock weathering was found to be the main process in the evolution of chemical composition of freshwater type, whereas the chemical structure of the low- and high-salinity types was primarily controlled by saltwater intrusion or anthropogenic activities.

1. Introduction

The chemical characteristics of groundwater are important factors determining its quality and utilization. The chemical composition of groundwater is controlled by many factors, including the mineralogy of aquifers, chemical composition of rainfall and surface water, climate, topography, and anthropogenic activities (Edmunds et al., 1982). The interaction of groundwater with these factors leads to the formation of different hydrogeochemical characteristics (Clark and Fritz, 1997). Therefore, identification of hydrogeochemical characteristics can further the understanding of the geochemical processes, hydrodynamics, and origin of groundwater as well as its interaction with aquifer materials (Furi et al., 2011). A great many hydrogeochemistry studies have been carried out to improve the understanding of groundwater systems; e.g., studies have been conducted in America (Quiroz Londoño et al., 2008; Oyarzún et al., 2013), Africa (Mojerezi et al., 2011), Europe (Dragon and Górski, 2009), and Asia (Sasamoto et al., 2011). The focus of this study is the Red River Delta (RRD) in Vietnam, where excessive groundwater withdrawal in the absence of the wise management and adequate understanding of the hydrogeochemical characteristics has caused serious problems, such as the unmitigated decline of groundwater levels and the deterioration of water quality (Bui et al., 2011).

The RRD is one of the largest deltas in Vietnam with an area of approximately 13,000 km^2. The delta, which encompasses the Vietnamese capital, Hanoi, had a population of approximately 20 million in 2012 (23% of Vietnam's total population), making it one

* Corresponding author.
E-mail address: nguyen-thanhthuy@ed.tmu.ac.jp (T.T. Nguyen).

http://dx.doi.org/10.1016/j.apgeochem.2015.07.009
0883-2927/

of Vietnam's most densely populated regions (Vietnam General Statistic Office, 2013). In terms of groundwater use, almost all communities located in the delta depend entirely on groundwater for their domestic water supply. Recently, due to the importance of groundwater in this region, several RRD groundwater-related studies have been carried out. Tran et al. (2012) undertook geophysical investigations to study the origin and extent of fresh groundwater, salty paleowaters, and recent saltwater intrusions in the RRD. Arsenic pollution of groundwater in the RRD has been investigated by various researchers such as Winkel et al. (2011), Berg et al. (2008), Jessen et al. (2008) and Agusa et al. (2005). In our earlier studies, we investigated the spatial characteristics of the aquifer system (Bui et al., 2011) as well as groundwater level trends in the entire RRD (Bui et al., 2012). To date, little information has been available regarding hydrogeochemical characteristics of the groundwater in the RRD with reference to major ion chemistry, especially the seasonal properties of hydrogeochemitry. The hydrogeochemical characteristics of groundwater in the two main aquifers of the RRD were also investigated by analyzing the physicochemical data from 31 conjunctive wells using classical hydrogeological and hydrochemical approaches (Piper and Gibbs diagrams) (Nguyen et al., 2014). Piper diagram was valuable in pointing out features of analyses of the hydrogeochemical data, but did not suffice to investigate the intrinsic relationships of data in the RRD. Therefore, it is necessary to apply the methods of clustering analysis for the hdyrogeochemical data in order to achieve a better understanding of the chemical properties of groundwater system in spaces as well as in time (Subyani and Al Ahmadi, 2009). Groundwater interacts with surface hydrologic systems, such as rivers, lakes, and oceans, and is indirectly influenced by seasonal changes during recharge and discharge. The annual cycle in groundwater levels in shallow aquifers was strongly governed by those of rainfall and river water level (Shamsudduha et al., 2009; Sanz et al., 2011). The change in seasons can potentially affect the hydrogeochemical properties of groundwater, especially in areas that have distinct dry and rainy seasons, such as Vietnam. Hence, investigation of the changes in the hydrogeochemical characteristics of groundwater in the RRD between the dry and rainy seasons (or vice versa) may reflect the groundwater hydrodynamics and circulation, and may help improve data collection programs for groundwater assessment, enabling better use of groundwater supplies.

In the RRD, the topmost Holocene unconfined aquifer (HUA) and the Pleistocene confined aquifer (PCA) are two important aquifers from which groundwater is being abstracted (Bui et al., 2011). Urban water systems predominately extract water from the PCA, whereas private households in rural areas pump groundwater from the HUA (Winkel et al., 2011). Since the wellheads of these private wells are not protected, groundwater contamination from domestic waste and agricultural sources can easily become widespread in the HUA of the rural areas, which lack proper domestic waste disposal facilities. In addition, pollution from the unconfined aquifer often spreads to deeper aquifers (Marghade et al., 2012). Therefore, hydrogeochemical studies of the unconfined groundwater in the RRD will provide a better understanding of possible changes in quality, and thus help to mitigate the inferior quality and provide guidance for the effective management of groundwater resources.

In order to identify the spatio-seasonal hydrogeochemical characteristics of groundwater, a robust classification scheme to cluster water chemistry samples into homogeneous groups is essential (Güler and Thyne, 2004). Several common clustering techniques have been utilized to divide groundwater samples into similar homogeneous groups (each representing a hydrogeochemical facies) with the ultimate objective of characterizing the quality of groundwater. These techniques include principal component analyses (Mojerezi et al., 2011), Q- and R-mode hierarchical cluster analysis (Reghunath et al., 2002), and the fuzzy c-means clustering technique (Güler and Thyne, 2004). These methods are efficient at grouping water samples by chemical similarities, but not useful for a visual assessment of the results or construction of maps showing hydrogeochemical facies (Güler et al., 2002). The recently proposed method of the self-organizing maps (SOM) is likely to become an alternative or complementary tool of those clustering methods (Iseri et al., 2009).

The SOM is a powerful technique capable of ordering multivariate data by similarity while preserving the topological structure of the data (Kohonen, 2001). Based on an unsupervised learning algorithm, the SOM has excellent visualization capabilities, including techniques that use the reference vectors of the SOM to provide an informative picture of the data (Hong et al., 2003). The SOM has been implemented in various aspects of water research, e.g., classification of environmental monitoring data (Jin et al., 2011) and clustering for wastewater treatment monitoring (Hilario and Ivan, 2004). The SOM has also proven to be a powerful and effective data analysis tool in meteorological analysis and detection of long-term climate changes (Nishiyama et al., 2007; Leloup et al., 2007). However, there have been very few published studies regarding the application of SOM to hydrogeochemical data for investigating the spatio-seasonal hydrogeochemical characteristics. This study attempted to apply SOM combined with a hierarchical cluster analysis to cluster unconfined groundwater chemistry data from the RRD.

The main objective of this study is to identify spatio-seasonal hydrogeochemical characteristics of unconfined groundwater in the RRD using SOM and Gibbs diagrams. In this study, Gibbs diagrams were aptly used to elucidate the cause and significance of the hydrogeochemical characteristics clustered by the SOM. Gibbs (1970) proposed chemical diagrams for assessing functional sources of dissolved chemical constituents and inferring the mechanism that controls the chemistry of surface water. Various researchers have demonstrated the usefulness of Gibbs diagrams for groundwater (Xiao et al., 2012; Oinam et al., 2012; Xing et al., 2013). The findings from this study will provide valuable insights into the spatio–seasonal hydrogeochemical characteristics of unconfined groundwater in the RRD.

2. Study area

The RRD is formed from the deposition of the sediment carried by a river during the Quaternary Ice Age including the Pleistocene and Holocene epochs. The Holocene sediments overlying the Pleistocene deposits, in which water seeps from the groundwater surface directly above the aquifer, are defined as an unconfined aquifer. Fig. 1 shows the geographical location of the entire RRD and the 47 groundwater sampling wells in the HUA, which are numbered from Well Nos. 1–31 and from 53 to 68 (Nos. 32–52 are for the PCA wells). In order to facilitate investigation of spatial hydrogechemical characteristics, the RRD was divided into three parts: upstream, middle-stream, and downstream by two lines, AA′ a006Ed BB′, as shown in Fig. 1. The two lines are the lines connecting boreholes of two typical hydrogeological cross-sections, which were created in our previous study (Bui et al., 2011). Well Nos. 1–15 and 53–57 are in the upstream area; Well Nos. 16–24 and 58–64 are in the middle-stream area; and Well Nos. 25–31 and 65–68 are in the downstream area. The RRD is the most-developed region in Vietnam and comprises 11 provinces and cities (Fig. 1). Two of Vietnam's major economic centers, Hanoi and Hai Phong, are located in the RRD (Bui et al., 2012).

The RRD is situated in the tropical monsoonal region with two distinct dry and rainy seasons. The rainy season starts in May and

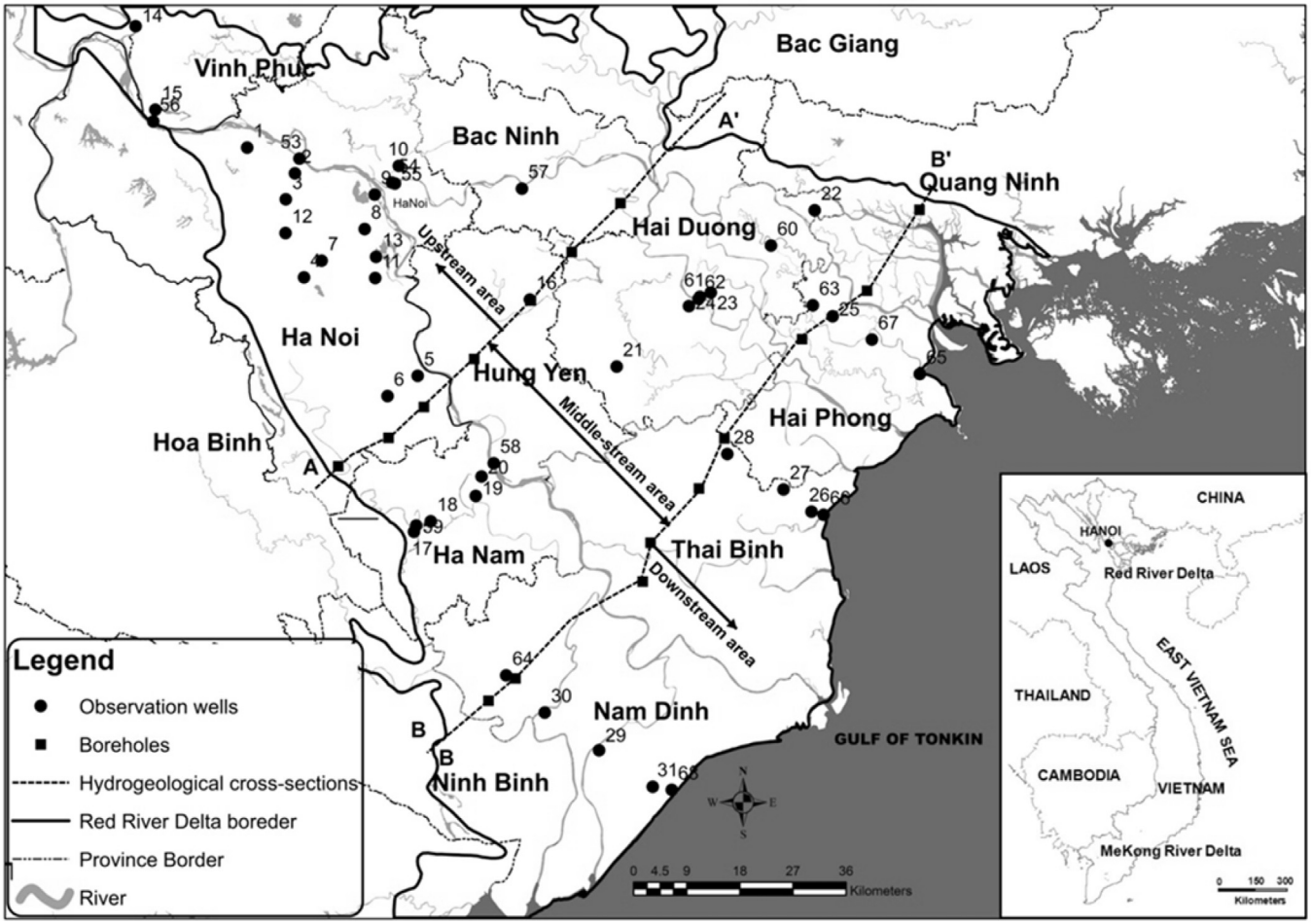

Fig. 1. The geographical location of the study area and location of the 47 sampling wells in the HUA.

ends in October, while the dry season lasts from November until April. The annual average rainfall is about 1600 mm. The annual average humidity is about 80%, and the average temperature is around 24 °C. The annual evaporation average is approximately 900 mm. The river network is quite extensive, with a network density of about 0.7 km/km^2 (Bui et al., 2011). The average discharge of the Red River at the Hanoi station, which was calculated from the daily discharge data from 1956 to 2010, is 3970 m^3/s during the rainy season and 1160 m^3/s during the dry season (IMHE-MONRE, 2011). The tidal range along the coast is approximately 4 m. The lakes, ponds, and canals in highly urbanized areas are seriously polluted with untreated domestic and industrial wastewater (Bui et al., 2012). Because groundwater is relatively cleaner and remains generally unaffected by the surface environmental problems, it has become the most trusted water source in the RRD (Bui et al., 2011).

In terms of regional geology, the RRD is composed of Quaternary-aged unconsolidated sediments with the thickness ranging from a few meters in the northwest to 150–200 m at the coastline in the southeast (Tran et al., 2012). The groundwater mostly exists as in the pores of the soil beneath the earth's surface that forms the topmost HUA and the PCA that forms the topmost HUA and the PCA, with the former having a high probability to be contaminated by pollutants from domestic as well as agricultural and industrial sources. Thus, the HUA will be the focus of this study. The HUA consists of silty clay and various sands mixed with gravel. The thickness of this layer varies up to more than 60 m, which increases from the northwest to southeast of the delta, whereas there exists a thin area with the thickness of less than 30 m in the middle of the delta (Bui et al., 2011). In general, the groundwater moves from northwest to southeast (from inland to the sea) following the general topography of the study area. The Red River is an important natural recharge source for groundwater storage in the RRD because it runs across HUA and in some places across PCA due to stream-bed erosion. The seasonality in groundwater levels for both HUA and PCA is closely associated with the annual cycles of river-water levels (Bui et al., 2012).

3. Materials and methods

3.1. Data used

The RRD has the most extensive hydrogeochemical database in Vietnam with a large number of data owners. However, the record lengths and intervals vary greatly depending on the completion time and the intended usage of the observation wells, as well as the aquifers and variables that are being monitored. In this study, we used the most recent groundwater chemical data from the National Hydrogeological Database Project (Tong, 2004), which were collected from 47 observation wells in the months of February (dry season) and August (rainy season) in 2011 to investigate the hydrogeochemical characteristics of HUA groundwater in the RRD.

Classification of chemical groundwater is based on the concentration of various major cations and anions or on the

interrelationships of ions. In our previous study (Nguyen et al., 2014), the Piper diagram was used to classify the major ions in the groundwater into various hydrogeochemical types to investigate and identify the hydrogeochemical facies of groundwater in the RRD. In this study, we also used the same kind of the chemical data consisting of major cations (Ca^{2+}, Mg^{2+}, Na^{+}, and K^{+}), and major anions (HCO_3^-, Cl^-, SO_4^{2-} and CO_3^{2-}) with total dissolved solids (TDS) so as to cluster and characterize the groundwater quality. The carbonate ion (CO_3^{2-}) concentration was calculated from the observed bicarbonate (HCO_3^-) concentration and pH data.

Standardization of the data was necessary prior to the application of the SOM to ensure that all values of the chemical parameters were given the same or similar importance. The results of the SOM application were sensitive to the data pre-processing method used, as the SOM is trained to be organized according to the Euclidean distances between input data. In this study, the range of the standardized values of the hydrogeochemical data for all parameters was 0–1, as given in the Eq (1):

$$x'_{ij} = \frac{x_{ij} - \min(x_j)}{\max(x_j) - \min(x_j)} \quad (1)$$

where x_{ij} is the concentration values of the chemical parameters of the ith wells.

This allows all the features to move in approximately the same ranges and therefore, they are treated by the SOM in a same way.

3.2. Methods

The SOM, developed by Kohonen (2001), is one kind of artificial neural network that is characterized by unsupervised training. It can project multi-dimensional, complex target data onto a two-dimensional regularly-arranged map in proportion to the degree of similarity (Jin et al., 2011). Therefore, it is an effective tool to visualize and explore data properties. In general, the objective of the SOM application is to obtain useful and informative reference vectors. These vectors can be acquired after iterative updates through the training of the SOM, which is composed of three main procedures: competition between nodes, selection of a winner node, and update of the reference vector.

Design of the SOM structure (calculation of the total number of nodes, side lengths), selection of a proper initialization method, and data transformation methods are very important features in the SOM application. The number of map nodes determines the accuracy and generalization capability of the SOM. According to the properties of the SOM, the bigger the map size is, the higher the resolution for pattern recognition, while the topographical adjacency is further among the clusters. A reasonable optimum solution of the compromise among the accuracy of pattern classification and topographical proximity of clusters to determine the number of the SOM nodes is the heuristic rule of $m = 5\sqrt{n}$, with m denoting the number of the SOM nodes and n representing the number of input data (Jin et al., 2011; Hentati et al., 2010; Jeong et al., 2010; Vesanto et al., 2000). In this study, this heuristic formula was used to determine the total number of nodes in the SOM. The ratio of the number of rows to the number of columns was calculated by the square root of the ratio between the two biggest eigenvalues of the transformed data (Hilario and Ivan, 2004).

After establishing the SOM structure, reference vectors for the SOM with the commonly used hexagonal array are initially set using the linear initialization method. In this study due to limited data, the linear initialization method was used, as it is more suitable for the pattern classification than the random initialization. The latter requires a large dataset and might cause boundary effects near the edges of the map (Jin et al., 2011; Hentati et al., 2010; Vesanto et al., 2000). In addition, the linear initialization approach can use eigenvalues and eigen vectors of the input data to set the initial reference vectors on the structured SOM. This means that the initial reference vectors already include prior information about the input data, resulting in an acceleration of the training phase (Jin et al., 2011; Vesanto et al., 2000). In this study, each reference vector was updated through the training process of the SOM using the batch mode, as given in Eqs. (2)–(4):

$$m_i(t+1) = \frac{\sum_{j=1}^{n} h_{ic}(t) x_j}{\sum_{j=1}^{n} h_{ic}(t)} \quad (2)$$

$$c = \mathrm{argmin}_k \{\|x_j - m_k\|\} \quad (3)$$

where, c is index of the BMU of data samples x_j and h_{ic} (t) is the weight of each data sample using the neighborhood function value-Gaussian, as shown in Eq. (4):

$$h_{ci}(t) = e^{\frac{-d_{ci}^2}{2\sigma_t^2}} \quad (4)$$

The reference vectors obtained at the end of the training process can be fine-tuned using cluster analysis methods. Various clustering algorithms are available in literature. These algorithms are generally classified into two types: hierarchical clustering and partitional clustering. These two clustering types can be integrated such that a result given by a hierarchical method can be improved via a partitional step, which refines via iterative relocation of points (Hilario and Ivan, 2004). In this study, both clustering algorithms were applied for the fine-tuning of the reference vectors. For the partitional clustering methods, the k-means algorithm is the most frequently used method for the SOM (Jin et al., 2011; Hentati et al., 2010; Nishiyama et al., 2007; Hilario and Ivan, 2004). The optimal number of clusters was selected by the Davies–Bouldin index (DBI) using the k-means algorithm, as shown in Eq. (5):

$$DBI = \frac{1}{N} \sum_{i=1, i\neq j}^{N} \max\left(\frac{\sigma_i + \sigma_j}{d(c_i, c_j)}\right) \quad (5)$$

Where, σ is standard deviation, N is number of clusters; σ_I, σ_j are the average distance of all patterns in cluster i,j to their cluster center c_I, c_j, respectively; and d (c_i, c_j) is the distance of cluster centers c_I and c_j. .

The DBI values were calculated from a minimum of 2 clusters to the total number of nodes. The calculation was based on the "similarity within a cluster" and "dissimilarity between clusters." Therefore, the number of clusters showing the minimum DBI was optimal for the trained SOM. For the hierarchical method, Ward's linkage method is the most commonly used approach (Jin et al., 2011; Hentati et al., 2010). In this study, a final fine-tuning cluster analysis was carried out by Ward's method using the optimal number of clusters.

To investigate the mechanisms governing the groundwater chemistry in the RRD, the chemical diagrams that were proposed by Gibbs (1970) were used to further evaluate the clustered data (wells). The weight ratios Na/(Na + Ca) and Cl/(Cl + HCO_3) were plotted against the total dissolved solids (TDS) separately on a logarithmic axis to represent the Gibbs cation and anion diagrams, respectively. The Gibbs diagrams were originally used to evaluate surface waters, but recent groundwater quality studies have used these diagrams to assess the sources of dissolved chemical constituents of groundwater (Marghade et al., 2012; Raju et al., 2011; Nagarajan et al., 2010).

4. Results and discussion

4.1. SOM and clustering results

The input data for the SOM application were varying concentrations of eight chemical parameters (major ions as described in Section 3.1) from 94 samples (n = 94), which were observed in 47 HUA wells during the dry and rainy seasons. Based on the methodology described above, the number of SOM nodes was calculated as 44, and the numbers of rows and columns were 11 and 4, respectively. The constructed SOM was used for the cluster analysis of the standardized groundwater chemistry monitoring data.

Fig. 2 shows the eight-component planes of SOM finally obtained after the training process. Each map represents the component value of the reference vectors for the 44 SOM nodes, in which the reference vectors were standardized to range 0–1, using shades of gray. The nodes that represent high values are dark gray and those representing low values are light gray. A comparison by means of a gradient of gray shades among the component SOMs can indicate informative and qualitative correlations among the studied parameters. Through visual investigation of the SOMs shown in Fig. 2, Mg^{2+}, Na^{+}, K^{+}, Cl^{-}, and SO_4^{2-} have similar gray gradients. This means that there is strong positive correlation among these five parameters. As can be seen in Fig. 2, the component map of Ca^{2+} shows weak positive correlation with other parameters suggesting that the change in Ca^{2+} concentration was independent upon changes in concentrations of other ions. The widespread of carbonate rock, which is the main source of Ca^{2+} along with the ion exchange reactions in the groundwater may be the reason of this weak correlation.

Table 1
Correlation coefficients among 8 physicochemical parameters.

	Ca^{2+}	Mg^{2+}	K^{+}	Na^{+}	HCO_3^{-}	SO_4^{2-}	Cl^{-}
Mg^{2+}	0.47						
K^{+}	0.44	0.996					
Na^{+}	0.43	0.996	0.998				
HCO_3^{-}	0.30	0.72	0.74	0.71			
SO_4^{2-}	0.54	0.89	0.86	0.87	0.46		
Cl^{-}	0.45	0.997	0.998	0.999	0.70	0.88	
CO_3^{2-}	0.10	0.67	0.69	0.67	0.95	0.46	0.66

Table 1 shows the correlation coefficients among eight physicochemical parameters using the standardized reference vectors. This table quantitatively confirms the strength of the relations between these parameters. For example, the relation of Cl^{-} with Mg^{2+}, K^{+}, Na^{+}, and SO_4^{2-} indicated significantly high correlation coefficients more than 0.88. CO_3^{2-} also showed a strong correlation with HCO_3^{-} with the correlation coefficient of 0.95, while the correlation coefficients of Ca^{2+} with other parameters were relatively low, as shown in Table 1.

In order to select the optimal number of clusters, the DBI values based on the k-means clustering algorithm were calculated for the minimum (2) to the maximum (44) possible clusters. Fig. 3 shows the variation of the DBI values after being applied to the data. The

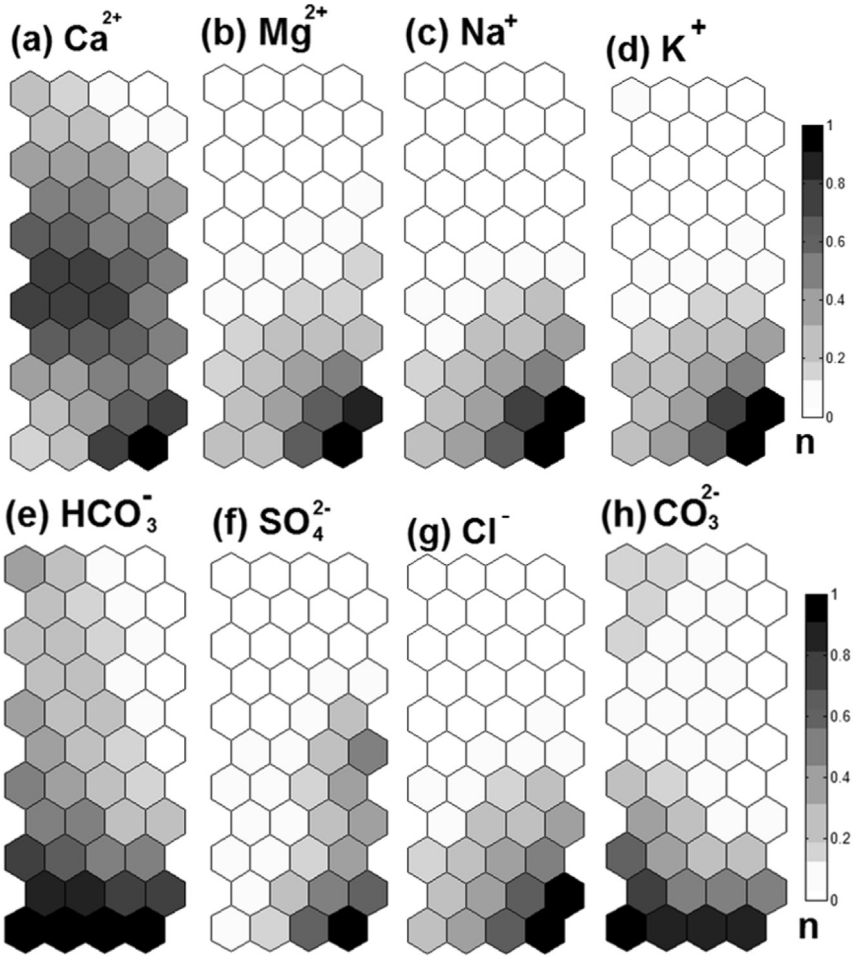

Fig. 2. Component planes for (a) Ca^{2+}, (b) Mg^{2+}, (c) Na^{+}, (d) K^{+}, (e) HCO_3^{-}, (f) SO_4^{2-}, (g) Cl^{-}, (h) CO_3^{2-}.

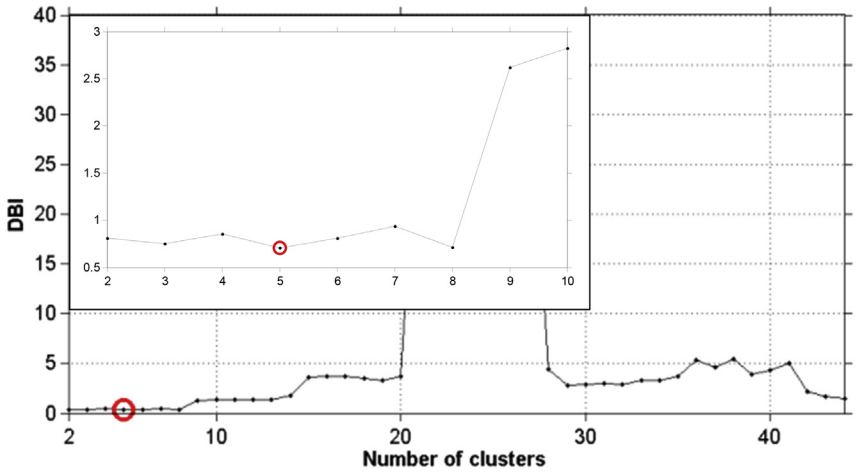

Fig. 3. Variation of DBI values with the optimal number of clusters marked by the circle on the figure.

most appropriate number of clusters corresponding to the minimum DBI was five. Once the optimum number of clusters had been selected, the hierarchical clustering algorithm using Ward's method was applied to obtain the five clusters for fine-tuning the pattern classification.

Fig. 4 shows the hierarchical cluster tree with the nodes of the SOM classified into five different clusters. The nodes in the SOM are numbered from top to bottom and from left to right. As shown in this figure, Clusters 1 and 5 have the smallest distance or highest similarity between clusters, implying that Clusters 1 and 5 have similar hydrogeochemical characteristics. In contrast, Cluster 4 and the other clusters are at relatively far distances, implying that the characteristics of Cluster 4 are different from the other clusters.

Fig. 5 shows the pattern classification map of the five clusters. The numbers represent Well Nos.; D and R denote the dry and rainy seasons; and u, m, and d denote upstream, middle-stream, and downstream areas, respectively. Simultaneous consideration of Fig. 2 (the component SOMs) and Fig. 5 indicates the type of data included in the respective clusters. For example, Cluster 4 (lower right part of Fig. 5) is associated with high-salinity water characterized by significantly high concentrations of all ions, which is observed in the same location of the respective component SOMs, as shown in Fig. 2. On the other hand, the groundwater samples in nodes with very low concentrations of almost all ions are located at the upper part of each SOM (classified as Cluster 1), as shown in Fig. 2.

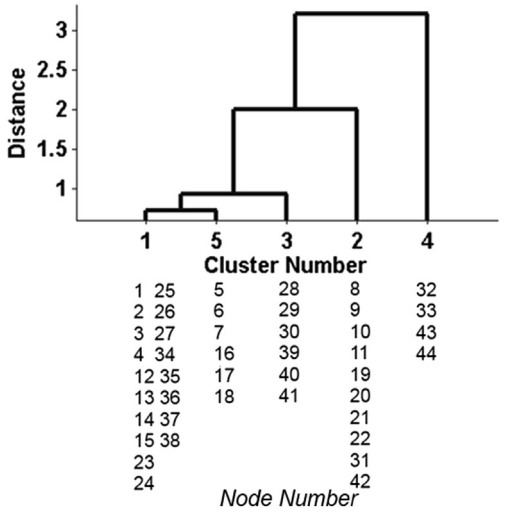

Fig. 4. Dendrogram with node numbers classified into the respective clusters.

4.2. Fundamental characteristics of the respective clusters

The reference vector values obtained from the SOM can provide quantitative information. In order to numerically characterize the classified data, the first quartile, median, and third quartile for the five clusters were calculated using the reference vectors. For instance, the quartiles for Cluster 1 were calculated using the standardized reference vectors of the 18 nodes classified into the cluster. Fig. 6 displays the radar charts of the eight parameters for the five clusters with the first quartile, median, and third quartile plotted. As shown in this figure, the visible patterns of Clusters 1 and 5 are similar (as mentioned above for Fig. 4). Both clusters reveal a pattern of low concentration of all the major ions. In particular, Cluster 1, with the lowest values for all major ions, represents the freshest water type. The highest values of all ions are classified into Cluster 4; therefore, the samples in this cluster can be assumed to be of the high-salinity type. Clusters 2 and 3 include relatively high values for all cations and Cl^-. Furthermore, Cluster 2 is associated with much higher anions of CO_3^{2-} and HCO_3^-. In this study, both Clusters 2 and 3 were classified as the low-salinity type, even though the distance between the clusters is quite far, as can be seen in Fig. 4. As mentioned above, groundwater in the RRD is mainly used for domestic water supply, drinking water and agriculture purposed. Therefore, from the practical point of views, the five classified clusters should be divided into three main water types on the basis of the similarity observed from the five radar charts in Fig. 6, in order to be more generalized and understandable for groundwater users and authorities in Vietnam. The freshwater type was associated with Clusters 1 and 3 due to the lowest values for all ions, as indicated in the upper and middle-left parts of Fig. 5. Cluster 4 was characterized by high concentrations of all major ions, representing the high-salinity type, as seen in the lower right of Fig. 5. The remaining two clusters (Clusters 2 and 3) are characteristic of the low-salinity type, as shown in the lower-left and middle-right parts of Fig. 5. In fact, to make the water users and authorities understand more easily, grouping clusters obtained from SOM has also been carried out in other studies (Jin et al., 2011). Table 2 shows the mean values calculated from the observed eight parameters for each cluster and the whole data. Clusters 1 and 5

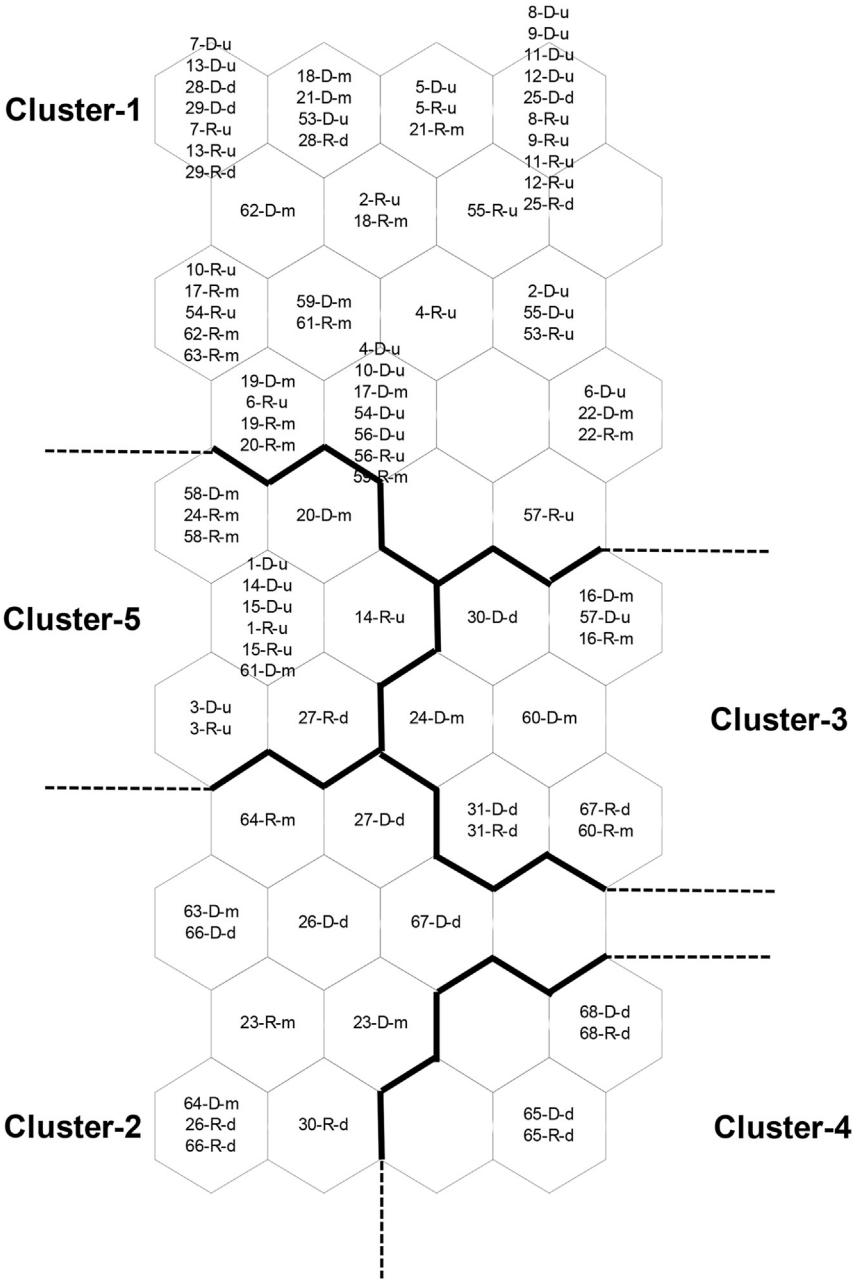

Fig. 5. Pattern classification map of the eight clusters by the SOM. Numbers represent the name of sampling wells in Fig. 1. The characters D and R correspond to the dry and rainy season. The last characters u, m, and d denote upstream, middle-stream, and downstream areas.

indicate lower mean values for almost all ions. Particularly Cluster 1 had the lowest values, except for CO_3^{2-}. These values confirm that Clusters 1 and 5 represent the freshwater type, as mentioned above. In contrast, Cluster 4 shows considerably higher mean values than those for the whole data for all major ions, indicating the most saline groundwater in the study area. Clusters 2 and 3 have relatively higher mean values for almost all ions compared to the values for the whole data.

4.3. Seasonal changes in the respective clusters

Fig. 7 displays the SOM, in which all the observation wells showing cluster changes from the dry to rainy seasons are indicated. From this figure, eight out of the 47 observation wells were observed to exhibit seasonal changes. Four wells (Well Nos. 24, 27, 57, and 63) showed changes of water types and the other four wells (Well Nos. 20, 30, 61, and 67) showed changes within the same water type.

Samples from each of the four wells that exhibited changes in water type changed from the low-salinity to the freshwater type. In other words, observation wells exhibited changes from the cluster with higher concentrations of most ions in the dry season to the cluster with lower concentrations in the rainy season. According to the previous study of Bui et al. (2011), HUA groundwater levels are usually situated within 4 m under the ground surface. Their annual cycle was strongly governed by those of rainfall and river water level with average amplitude of about 2 m. In addition, groundwater near the Red River receives mostly recharges from surface

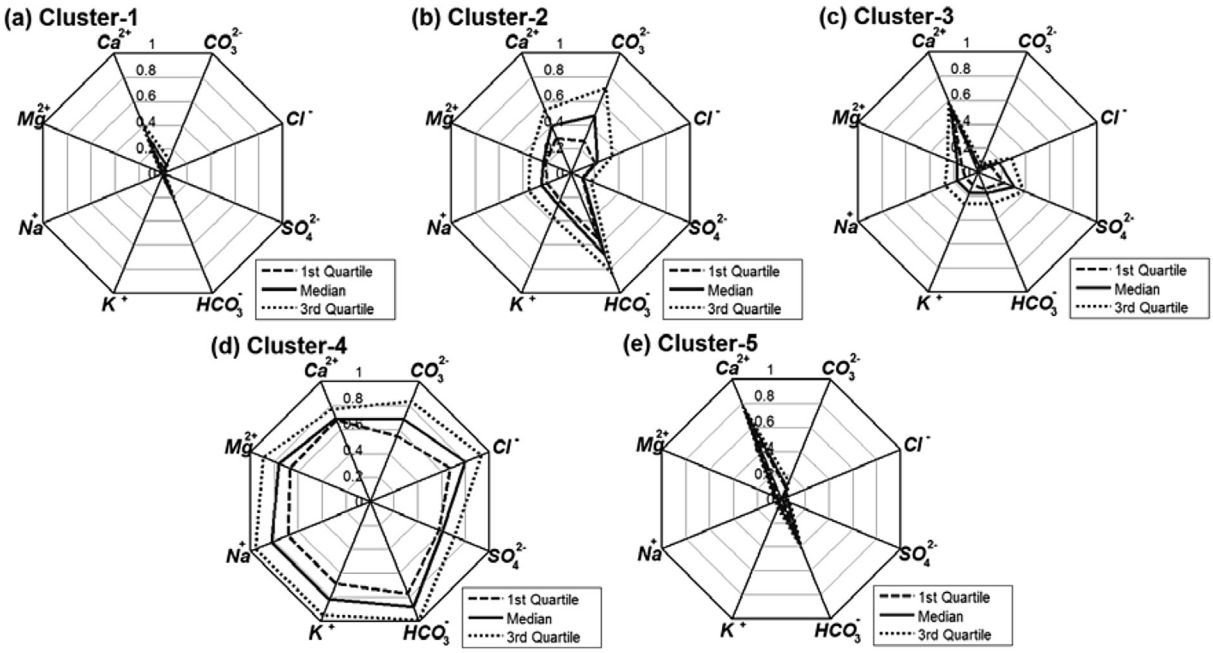

Fig. 6. Radar charts for the respective clusters with the first quartile (dashed lines), median (solid lines) and the third quartile (dotted lines) by obtained reference vectors.

Table 2
Mean values of eight parameters for the five clusters and whole data.

Mean	Ca^{2+} (mg/L)	Mg^{2+} (mg/L)	Na^{+} (mg/L)	K^{+} (mg/L)	HCO_3^- (mg/L)	SO_4^{2-} (mg/L)	Cl^- (mg/L)	CO_3^{2-} (mg/L)
Cluster 1	70	31	78	6	366	23	135	0.026
Cluster 2	70	172	1330	58	911	85	2190	0.138
Cluster 3	105	154	1310	46	301	352	2310	0.010
Cluster 4	156	779	6800	256	1050	771	7620	0.179
Cluster 5	138	52	108	11	587	49	192	0.031
Whole data	88	97	659	28	491	102	1130	0.046

water because shallow aquifers adjacent to river mostly experience great groundwater recharge. The increase of groundwater recharge, e.g., from rainfall and rivers, may create a dilution effect, which could explain the downward trends in the ion concentrations during the rainy season.

In terms of changes in clusters within the same water type, samples from Well No. 30 notably changed from Cluster 3 (the low-salinity type with relatively high SO_4^{2-} and low CO_3^{2-} and HCO_3^-) to Cluster 2 (the low-salinity type with high CO_3^{2-} and HCO_3^-), while Well No. 67 changed from Cluster 2 to Cluster 3. As shown in Fig. 1, Well No. 30 is located in the southwest downstream area, whereas Well No. 67 is situated in the northeast downstream area. According to Bui et al. (2012), the HUA in the RRD is recharged primarily from rivers and the surrounding mountains. The western mountains are carbonate rock formations consisting of marble, limestone, and dolomite, whereas sulfate minerals (gypsum and anhydrite) are commonly found in the northeast mountain area (Drogue et al., 2000). This suggests that the increase of groundwater recharge from the mountains during the rainy season, which causes increased concentrations of carbonate in Well No. 30 and sulfate in Well No. 67, could be the reason for these changes. On the other hand, samples from Well Nos. 20 and 61 changed from Cluster 5 to Cluster 1 (the lowest salinity). This may be due to the increase of groundwater recharge by surface water, such as rainfall, lakes or rivers, during the rainy season.

In our former study (Nguyen et al., 2014), we used Piper diagram to investigate the seasonal changes in hydrogeochemical facies. However, some of the seasonal changes in water types as well as clusters within the same water type, which were obtained by using SOM, were not detected by using Piper diagram. For example, samples in Well Nos. 27 showed seasonal changes of water types (from low-salinity type to freshwater type) as mentioned above, but Piper diagram showed that groundwater in these wells was the [Na^+-Cl^-] ion type in both season. Similarly, samples in Well Nos. 20 and 30, which showed the seasonal changes in clusters within the same water type, were the [Ca^{2+}-HCO_3^-] and [Na^+-Cl^-] ion types, respectively.

Furthermore, it is difficult for Piper diagram to visually detect the seasonal changes in ion types because of many overlapped samples plotted in Piper diagram, especially when the amount of data increases. On the other hand, SOM can distinctly visualize the seasonal changes as plotting in the different nodes, as well as how big the changes were in a manner more easily by distances between the nodes of samples in both seasons.

4.4. Spatial distribution of the respective clusters

Fig. 8 shows the spatial distribution of the five clusters classified by the SOM in the RRD. The symbols circle, triangle, cross star, and square represent Clusters 1–5, respectively. The white and black colors correspond to the dry and rainy seasons, respectively. As seen in Fig. 8, Cluster 4 (the high-salinity type) is observed in the coastal area, e.g., Well Nos. 65 and 68. Saltwater intrusion could be the reason for the presence of the high-salinity type in the coastal area.

Besides the fact that Clusters 2 and 3, characterized by the low-salinity type, are observed in the downstream area (Well Nos. 26,

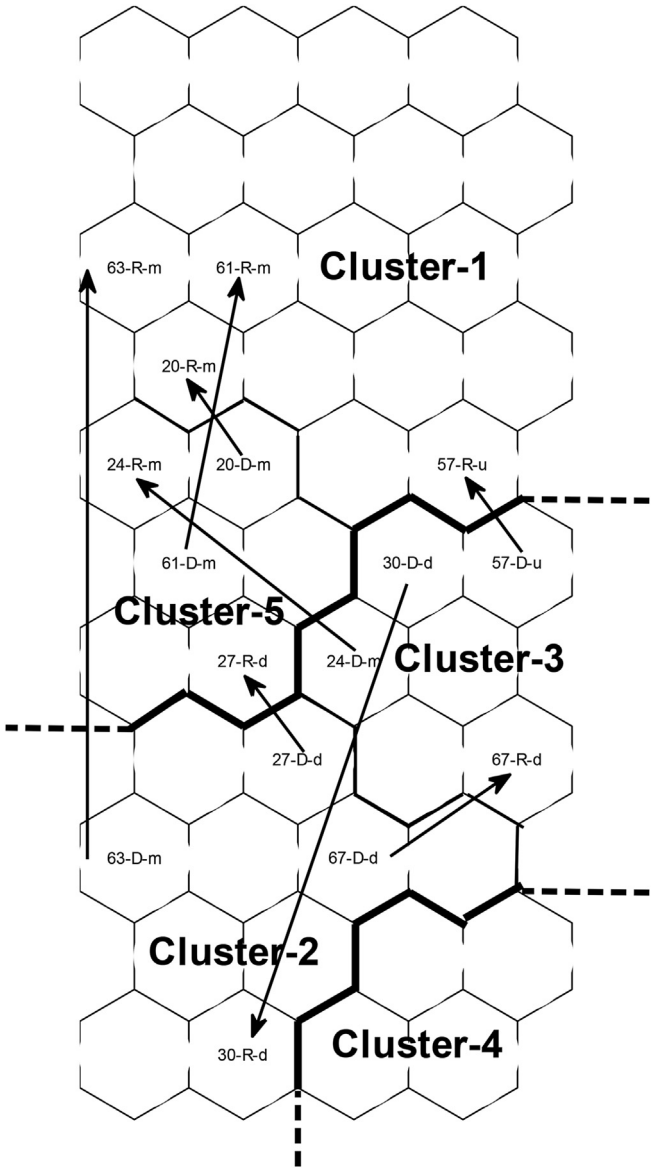

Fig. 7. Representation of the sampling points showing the changes in clusters from the dry to the rainy seasons. The super-bold line outlines water types.

27, 30, and 66), they are also found in the northeast part of the upstream and middle-stream areas (Well Nos. 16, 23, 24, 57, 60, and 63). Especially, Cluster 3 (the low-salinity type with relatively high SO_4^{2-}) was found in the northeast part of the delta. This finding is consistent with the previous study of Jessen et al. (2008), but not detected in our previous study by using Piper diagram (Nguyen et al. (2014) and the study of Tran el al. (2012), which were based on the geophysical investigation. Along the Red River and its tributaries, salty bottom water is transported as far inland as 35 km from the sea (Vu, 1996). This salty bottom water may leak into adjacent aquifers, either as a density-driven flow or as a downward flow controlled by a hydraulic gradient, where the river bottom sediments are highly permeable. Therefore, the low-salinity type found in the downstream is probably due to saltwater intrusion from the river. On the other hand, upon the closer inspection of land use, Well Nos. 16, and 57 (northeast part of the upstream area) are located in an intensely irrigated agricultural area (Asian Development Bank, 2000). Thus, it is reasonable to infer that the presence of the low-salinity type in the upstream and middle-stream areas could be influenced by agricultural activities. The presence of stagnant saline water in the estuarine clay units for the Holocene aquifer from the mid-Holocene marine sediments (Jessen et al., 2008) could be the reason of the presence of the low-salinity type in the middle-stream area (Well Nos. 23, 24, 60, and 63).

Clusters 1 and 5, representing the freshwater type, are found not only in the upstream and middle-stream areas but also in the downstream area, as seen in Well Nos. 27, 28 (northeast of the downstream area) and 29 (south of the downstream area). The presence of the freshwater type in the northeast of the downstream area implies that saltwater intrusion does not affect groundwater this far inland. On the other hand, Wagner et al. (2012) identified a local lens of freshwater existing in the south portion of the downstream area, which explains the presence of the freshwater type found in Well No. 29. The existence of freshwater type in the downstream area was not obtained by using Piper diagram as in our previous study (Nguyen et al., 2014).

The objective of using Piper diagram is neither to cluster the hydrogeochemical data to discover absorbing characteristics nor to find a new set of water types, but rather to decide how the hydrogeochemical data should be classified into different ion types. Furthermore, Piper diagram just classifies the water ion types into the combination of one of three cation types and one of three antion types, whereas application of SOM can flexibly cluster the hydrogeochemical data into any combination among 8 cation and anion parameters by the automated process. Therefore, application of Piper diagram did not suffice to investigate the intrinsic relationship between each parameter of the hydrogeochemical data.

The samples showing cluster changes from the dry to the rainy seasons were primarily located in the middle-stream and downstream areas of the delta. This suggests that surface water strongly influences the chemical characteristics of unconfined groundwater at the middle-stream and downstream areas of the delta, but weakly influences the upstream area during the rainy season.

4.5. Factors governing water chemistry

Fig. 9 shows the Gibbs diagrams for the five clusters classified by the SOM. The symbols representing Clusters 1–5 in this figure are the same as those in Fig. 8. Gibbs (1970) found that most of the world's surface water falls within the boomerang-shaped boundaries. Based on analytical chemical data for numerous surface samples, Gibbs theorized that three major mechanisms control world surface water chemistry. These mechanisms can be classified into three domains: precipitation dominance (lower part), rock dominance (middle part), and evaporation dominance (upper part), as shown in Fig. 9. Clusters 1 and 5 (the freshwater type) were plotted toward the rock dominance domain due to low TDS. Some samples in these clusters fell toward the evaporation dominance domain but no sample fell in the precipitation dominance domain. This suggests that Clusters 1 and 5 are dominated by rock mineral dissolution processes.

On the other hand, Cluster 4 (the high-salinity type) was plotted in the evaporation dominance domain with the highest TDS and significantly high ratios of $Na/(Ca + Na)$ and $Cl/(Cl + HCO_3)$. The high TDS is due to high concentrations of all ions (as shown in Table 2). This suggests saltwater intrusion is the main factor affecting the groundwater chemistry of this cluster. Furthermore, Clusters 2 and 3 (the low-salinity type) had relatively high TDS and high ratios of $Na/(Ca + Na)$ and $Cl/(Cl + HCO_3)$, and thus, they fell in the evaporation dominance domain. Anthropogenic and marine activities, such as intensive and long-term irrigation, agricultural fertilizers, and saltwater intrusion, could be the primary factors causing these clusters to fall into the evaporation dominant domain.

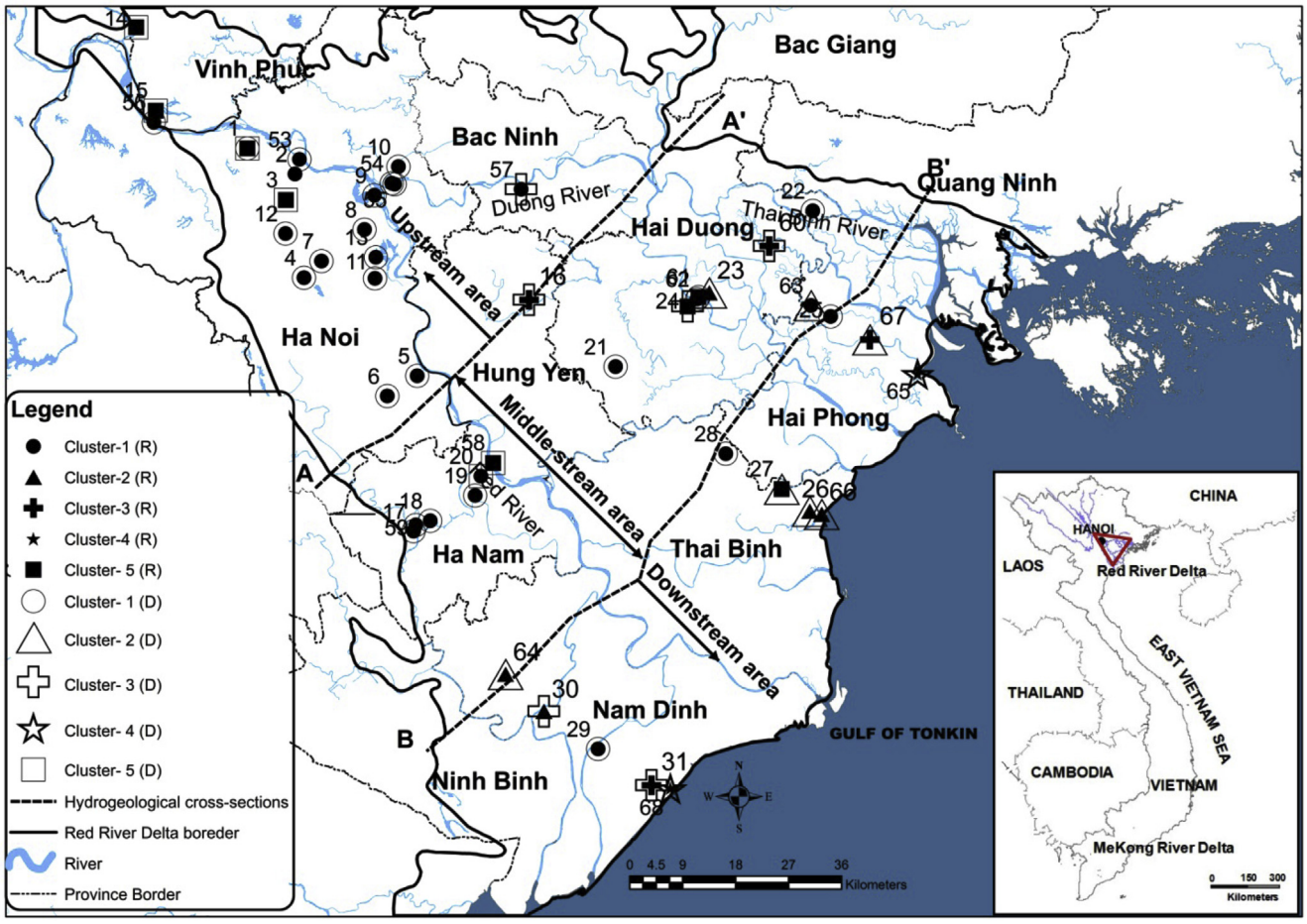

Fig. 8. Spatial distribution of the respective clusters.

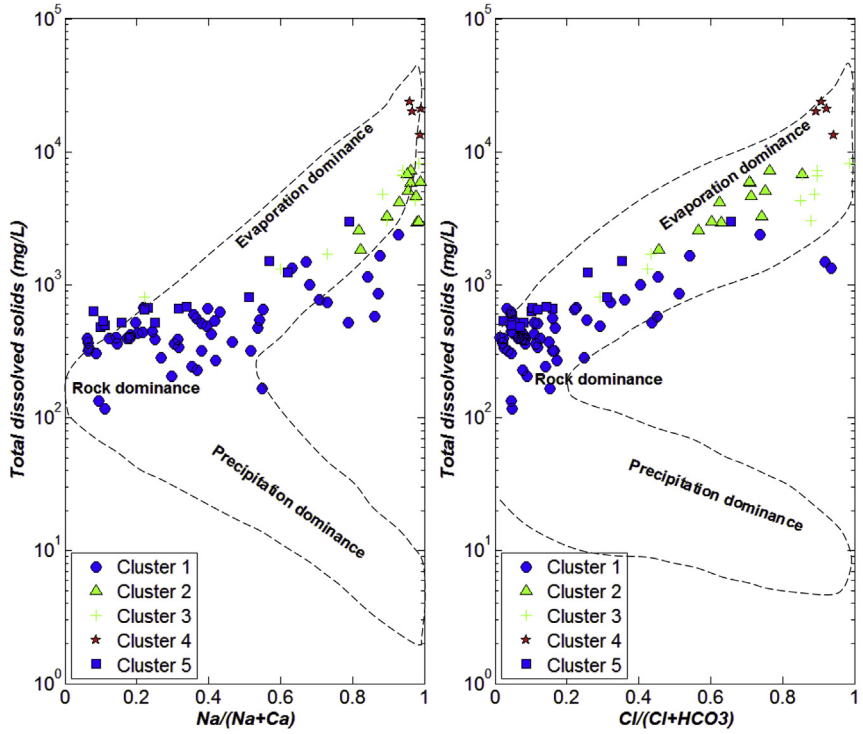

Fig. 9. Gibbs diagrams for the classified data into the respective cluster.

5. Conclusions

The main objective of this study was to identify the spatio-seasonal hydrogeochemical characteristics of unconfined groundwater of the RRD. In this paper, hydrogeochemical parameters (major ions) from 47 HUA observation wells in the RRD acquired during the dry and rainy seasons in 2011 were classified using the SOM in combination with a hierarchical cluster analysis. In addition, Gibbs diagrams were created to elucidate the hydrogeochemical characteristics classified by the SOM.

From the results of the SOM application, the groundwater chemistry data were divided into five clusters. From the practical point of view, these five clusters revealed three basic representative water types characterized by the high salinity (Cluster 4), low salinity (Clusters 2 and 3) and freshwater (Clusters 1 and 5). The high-salinity type was located in the coastal area, whereas the low-salinity type samples were found not only in the downstream area but also in the northeastern parts of the upstream and middle-stream areas, where groundwater samples were mainly classified into Cluster 3. With closer inspection of land use, the groundwater of this cluster was considered to be contaminated by agricultural activities. The freshwater type was generally found in the upstream and middle-stream areas. However, some samples belonging to this type were also found in the northeastern and southern parts of the downstream area.

Cluster changes from the dry to rainy seasons were detected in approximately one-fifth of the observation wells, mostly found in the middle-stream and downstream areas. This suggests strong influence of surface water on the chemical characteristics of unconfined groundwater at the middle-stream and downstream areas of the delta during the rainy season.

The results of the Gibbs diagrams suggest that rock weathering is the main process in the evolution of chemical composition of groundwater characterized by the freshwater type, whereas the chemical structure of the groundwater representing the low- and high-salinity types is primarily controlled by saltwater intrusion or anthropogenic activities.

Acknowledgments

This study was carried out as a part of the research project “Solutions for the water related problems in Asian metropolitan areas” supported by the Tokyo Metropolitan Government, Japan (represented by Akira Kawamura). We would like to thank the Department of Geology and Minerals of Vietnam for supplying the necessary field data from the earlier feasibility studies.

References

Agusa, T., Inoue, S., Kunito, T., Tu, B.M., Pham, T.K.T., Subramanian, A., Iwata, H., Pham, H.V., Tanabe, S., 2005. Widely distributed arsenic pollution in groundwater in the Red River Delta, Vietnam. Biomed. Res. Trace Elem. 16, 296–298.

Asia Development Bank, 2000. Final Report on Management Study on Land Use and Water Management, Red River Basin Water Resources Management Project. Available via. http://bicn.com/wei/resources/Bennett-2000-ADBTA-2871-VIE-Land-Use-Water-Management-RRB.pdf.

Berg, M., Stengel, C., Pham, T.K.T., Pham, V.H., Sampson, M.L., Leng, M., Samreth, S., Fredericks, D., 2008. Hydrological and sedimentary controls leading to arsenic contamination of groundwater in the Hanoi area, Vietnam: the impact of iron-arsenic ratios, peat, river bank deposits, and excessive groundwater abstraction. Chem. Geol. 249, 91–112.

Bui, D.D., Kawamura, A., Tong, T.N., Amaguchi, H., Nakagawa, N., Iseri, Y., 2011. Identification of aquifer system in the whole Red River Delta, Vietnam. Geosci. J. 15 (3), 323–338.

Bui, D.D., Kawamura, A., Tong, T.N., Amaguchi, H., Nakagawa, N., 2012. Spatio-temporal analysis of recent groundwater-level trends in the Red River Delta, Vietnam. Hydrogeol. J. 20, 1635–1650.

Clark, I.D., Fritz, P., 1997. Environmental Isotopes in Hydrogeology. Lewis Publisher, Boca Raton, p. 328.

Dragon, K., Górski, A.J., 2009. Identification of hydrogeochemical zones in postglacial buried valley aquifer (Wielkopolska Buried Valley aquifer, Poland). Environ. Geol. 58, 859–866.

Drogue, C., Cat, N.N., Dazy, J., 2000. Geological factors affecting the chemical characteristics of the thermal waters of the carbonate karstified aquifers of Northern Vietnam. Hydrol. Earth Syst. Sci. 4 (2), 332–340.

Edmunds, W.M., Bath, A.H., Miles, D.L., 1982. Hydrochemical evolution of the East Midlands Triassic sandstone aquifers, England. Geochim. Cosmochim. Acta 15, 737–752.

Furi, W., Razack, M., Abiye, T.A., Kebede, S., Legesse, D., 2011. Hydrochemical characterization of complex volcanic aquifers in a continental rifted zone: the Middle Awash basin, Ethiopia. Hydrogeol. J. 20, 385–400.

Gibbs, R.J., 1970. Mechanisms controlling world water chemistry. Science 17, 1088–1090, 1970.

Güler, C., Thyne, G.D., McCray, J.E., Turner, A.K., 2002. Evaluation of graphical and multivariate statistical methods for classification of water chemistry data. Hydrogeol. J. 10, 455–474.

Güler, C., Thyne, G.D., 2004. Delineation of hydrochemical facies distribution in a regional groundwater system by means of fuzzy c-means clustering. Water Resour. Res. 40 http://dx.doi.org/10.1029/2004WR003299.

Hentati, A., Kawamura, A., Amaguchi, H., Iseri, Y., 2010. Evaluation of sedimentation vulnerability at small hillside reservoirs in the semi-arid region of Tunisia using the Self-Organizing Map. Geomorphology 122, 56–64.

Hilario, L.G., Ivan, M.G., 2004. Self-organizing map and clustering for wastewater treatment monitoring. Eng. Appl. Artif. Intel. 17, 215–225.

Hong, Y.T., Rosen, M.R., Bhamidimarri, R., 2003. Analysis of a municipal wastewater treatment plant using a neural network-based pattern analysis. Water Res. 37, 1608–1618.

IMHE-MONRE, 2011. Annual Report on Hydrological Observation in Vietnam. Vietnamese Ministry of Environment and Natural Resources.

Iseri, Y., Matsuura, T., Iizuka, S., Nishiyama, K., Jinno, K., 2009. Comparison of pattern extraction capability between self-organizing maps and principal component analysis. Mem. Fac. Eng. Kyushu Univ. 69 (2), 37–47. http://kenkyo.eng.kyushu-u.ac.jp/memoirs-eng/bulletin/69/2/paper2.pdf.

Jessen, S., Larsen, F., Postma, D., Pham, H.V., Nguyen, T.H., Pham, Q.N., Dang, D.N., Mai, T.D., Nguyen, T.M.H., Trieu, D.H., Tran, T.L., Dang, H.H., Jakobsen, R., 2008. Palaep-hydrogeological control on groundwater as levels in Red River Delta, Vietnam. Appl. Geochem. 23, 3116–3126.

Jeong, K.S., Hong, D.G., Byeon, M.S., Jeong, J.C., Kim, H.G., 2010. Stream modification patterns in a river basin: field survey and self-organizing map (SOM) application. Ecol. Inf. 5, 293–303.

Jin, Y.H., Kawamura, A., Park, S.C., Nakagawa, N., Amaguchi, H., Olsson, J., 2011. Spatiotemporal classification of environmental monitoring data in the Yeongsan River basin, Korea, using self-organizing maps. J. Environ. Monit. 13, 2886–2894.

Kohonen, T., 2001. Self-organizing Maps, third ed. Springer.

Leloup, J.A., Lachkar, Z., Boulanger, J.P., Thiria, S., 2007. Detecting decadal changes in ENSO using neural networks. Clim. Dyn. 28, 147–162.

Marghade, D., Malpe, D.B., Zade, A.B., 2012. Major ion chemistry of shallow groundwater of a fast growing city of Central India. Environ. Monit. Assess. 184, 2405–2418.

Mojerezi, M., Vogt, R.D., Aagaard, P., Saka, J.D.K., 2011. Hydro-geochemical processes in an area with saline groundwater in lower Shire River valley, Malawi: an integrated application of hierarchical cluster and principal component analyses. Appl. Geochem. 26, 1399–1413.

Nagarajan, R., Rajmohan, N., Mahendran, U., Senthamilkumar, S., 2010. Evaluation of groundwater quality and its suitability for drinking and agricultural use in Thanjavur city, Tamil Nadu, India. Environ. Monit. Assess. 171, 289–308.

Nishiyama, K., Endo, S., Jinno, K., Uvo, C.B., Olsson, J., Berndtsson, R., 2007. Identification of typical synoptic patterns causing heavy rainfall in the rainy season in Japan by a self-organizing map. Atmos. Res. 83, 185–200.

Nguyen, T.T., Kawamura, A., Tong, N.T., Nakagawa, N., Amaguchi, H., Gilbuena, R., 2014. Hydrogeochemical characteristics of groundwater from the two main aquifers in the Red River Delta, Vietnam. J. Asian Earth Sci. 93, 180–192.

Oinam, J.D., Ramanathan, A.L., Singh, G., 2012. Geochemical and statistical evaluation of groundwater in Imphal and Thoubal district of Manipur, India. J. Asian Earth Sci. 48, 136–149.

Oyarzún, J., Carvajal, M.J., Maturana, H., Núnez, J., Kretschmer, N., Amezaga, J.M., Rotting, T.S., Strauch, G., Thyne, G., Oyarzún, R., 2013. Hydrochemical and isotopic patterns in a calc-alkaline Cu- and Au- rich arid Andean basin: the Elqui River watershed, North Central Chile. Appl. Geochem. 33, 50–63.

Quiroz Londoño, O.M., Martínez, D.E., Dapeña, C., Massone, H., 2008. Hydrogeochemistry and isotope analyses used to determine groundwater recharge and flow in low-gradient catchments of the province of Buenos Aires, Argentina. Hydrogeol. J. 16, 1113–1127.

Raju, N.J., Shukla, U.K., Ram, P., 2011. Hydrogeochemistry for the assessment of groundwater quality in Varanasi: a fast-urbanizing center in Uttar Pradesh, India. Environ. Monit. Assess. 173, 279–300.

Reghunath, R., Sreedhara Murthy, T.R., Raghavan, B.R., 2002. The utility of multivariate statistical techniques in hydrogeochemical studies: an examples from Karnataka, India. Water Res. 36, 2437–2442.

Sanz, D., Castano, S., Cassiraga, E., et al., 2011. Modeling aquifer-river interactions under the influence of groundwater abstraction in the Mancha Oriental System (SE Spain). Hydrogeol. J. 1, 475–487.

Sasamoto, H., Arthur, R.C., Hama, K., 2011. Interpretation of undisturbed hydrogeochemical conditions in Neogene sediments of the Horonobe area, Hokkaido,

Japan. Appl. Geochem. 26, 1454–1477.
Shamsudduha, M., Chandler, R.E., Taylor, R.G., et al., 2009. Recent trends in groundwater levels in a highly seasonal hydrological system: the Ganges–Brahmaputra–Meghma Delta. Hydrol. Earth Syst. SC 13, 273–2385.
Subyani, A.M., Al Ahmadi, M.E., 2009. Multivariate statistical analysis of groundwater quality in Wadiranyah, Saudi Arabia. JAKU Earth Sci. 21 (2), 29–46.
Tong, T.N., 2004. National Hydrogeology Database Program. Final Project Report. Department of Geology and Minerals of Vietnam, p. 120 (in Vietnamese).
Tran, T.L., Larsen, F., Pham, Q.N., Christiansen, A.V., Tran, N., Vu, V.H., Tran, V.L., Hoang, V.H., Hinsby, K., 2012. Origin and extent of fresh groundwater, salty paleowaters and recent saltwater intrusions in Red River flood plain aquifers, Vietnam. Hydrogeol. J. 20, 1295–1313.
Vesanto, J., Himberg, J., Alhoniemi, E., Parahankangas, J., 2000. SOM Toolbox for Matlab 5. Helsinki Univeriity Report A57.
Vietnam General Statics Office, 2013. Statistical Handbook of Vietnam. General Statics Office, Hanoi. Available via. http://www.gso.gov.vn (accessed 27.12.13.).
Vu, T.C., 1996. Salinity intrusion in the Red River Delta. In: Seminar on Environment and Development in Vietnam, Canberra, 6–7 December 1996. Available via. http://coombs.anu.edu.au/~vern/env_dev/papers/pap08.html (accessed 28.12.12.).
Wagner, F., Ludwig, R.R., Noell, U., Hoang, H.V., Pham, Q.N., Larsen, F., Lindenmaier, F., 2012. Genesis of economic relevant fresh groundwater resources in Pleistocene/Neogene aquifers in Nam Dinh (Red River Delta, Vietnam). EGU General Assem. 14, 2273.
Winkel, L.E., Pham, T.K.T., Vi, M.L., Stengel, C., Amini, M., Nguyen, T.H., Pham, H.V., Berg, M., 2011. Arsenic pollution of groundwater in Vietnam exacerbated by deep aquifer exploitation for more than a century. PNAS Early Edition 1–6 PNAS 108 (4), 1246–1251. Washington, DC.
Xiao, J., Jin, Z.D., Zhang, F., Wang, J., 2012. Solute geochemistry and its sources of the groundwaters in the Qinghai Lake catchment, NW China. J. Asian Earth Sci. 52, 21–30.
Xing, L., Guo, H., Zhan, Y., 2013. Groundwater hydrochemical characteristics and processes along flow paths in the North China Plain. J. Asian Earth Sci. 70–71, 250–264.